

# A Study of Data Rate Equivalent UW-OFDM and CP-OFDM Concepts

Christian Hofbauer, *Student Member, IEEE*, Mario Huemer, *Senior Member, IEEE*,  
Klagenfurt University, Institute of Networked and Embedded Systems  
Universitaetsstr. 65-67, A-9020 Klagenfurt, {chris.hofbauer, mario.huemer}@aau.at

**Abstract**—Unique word – orthogonal frequency division multiplexing (UW-OFDM) is a novel transmit signal structure for OFDM where the usual cyclic prefixes (CPs) are replaced by deterministic sequences, the so-called UWs. Since unique words represent known sequences, they can advantageously be used for synchronization and estimation tasks, but also for improving the bit error ratio (BER) behavior of an UW-OFDM system. Recent research results have demonstrated the superior BER behavior of UW-OFDM over conventional CP-OFDM used for real-world communication systems, e.g. for the IEEE 802.11a WLAN standard. In this paper we extend these investigations by considering different and data rate equivalent UW-OFDM and CP-OFDM configuration setups. We show simulation results for various frequency selective environments and additionally compare UW-OFDM with UW based single carrier/frequency domain equalization (UW-SC/FDE) systems.

**Index Terms**—Cyclic Prefix (CP), non-systematic coded Unique Word OFDM (UW-OFDM), Unique Word based Single Carrier/Frequency Domain Equalization (UW-SC/FDE)

## I. INTRODUCTION

In [1]-[3] we proposed an OFDM (orthogonal frequency division multiplexing) signaling scheme, where the usual cyclic prefixes (CPs) [4] are replaced by deterministic sequences, that we call unique words (UWs). A related but – when regarded in detail – also very different scheme is KSP (known symbol padded)-OFDM [5]. Fig. 1a – 1c compare the CP-, KSP-, and UW-based OFDM transmit data structures. In CP- as well as in UW-OFDM the linear convolution of the transmit signal with the channel impulse response is transformed into a cyclic convolution. However, different to the CP, the UW is part of the DFT (discrete Fourier transform)-interval as indicated in Fig. 1. Furthermore, the CP is a random sequence, whereas the UW is deterministic. Hence, the UW can optimally be designed for particular needs like synchronization and/or channel estimation purposes at the receiver side. The broadly known KSP-OFDM uses a structure similar to UW-OFDM, since the known symbol (KS) sequence is deterministic as well. The most important difference between KSP- and UW-OFDM is the fact, that the UW is part of the DFT interval, whereas the KS is not. On the one hand this characteristic of the UW implies the cyclic convolution property addressed above, and

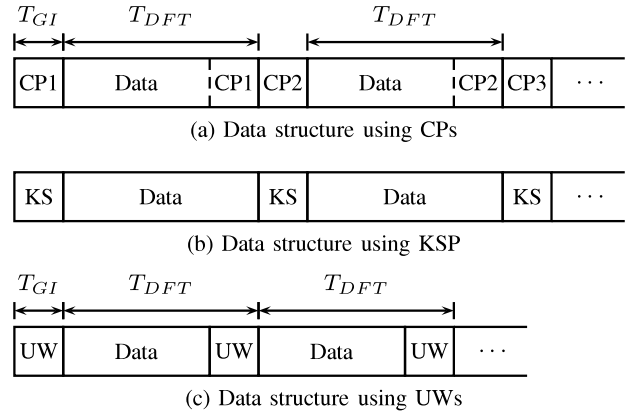


Fig. 1. Transmit data structure using a CP (a), a KS (b) or a UW (c).

on the other hand, but no less importantly, the insertion of the UW within the DFT-interval introduces correlations in the frequency domain, which can advantageously be exploited by the receiver to improve the BER (bit error ratio) performance. Whilst in both schemes the deterministic sequences can be used for synchronization and channel estimation purposes, KSP-OFDM does not feature these correlations in frequency domain.

In the concept described in [1]-[3] we suggested to generate UW-OFDM symbols by appropriately loading so-called redundant subcarriers. Hence, we obtain an OFDM symbol which consists of dedicated data and additionally of dedicated redundant subcarriers. As such, these OFDM symbols can be considered as a systematic code, thus leading to the idea of systematic coded UW-OFDM.

In [6] we introduced a new concept which we refer to as *non-systematic coded UW-OFDM*. Here, we can no longer speak of dedicated data and redundant subcarriers, but both, data and redundancy symbols, are spread over several subcarriers. We thus obtain OFDM symbols representing a non-systematic code. It turns out that the non-systematic case by far outperforms the systematic coded concept. Consequently, in this paper we will focus on non-systematic coded UW-OFDM.

Up till now, all performance comparisons of UW-OFDM with conventional CP-OFDM have been focusing on adopting the UW-OFDM system as closely as possible to the IEEE 802.11a WLAN standard. We used the same sampling frequency, DFT size, subcarrier spacing and also introduced

This work was supported by the Austrian Science Fund (FWF): I683-N13.  
Copyright (c) 2012 IEEE. Personal use of this material is permitted. Permission from IEEE must be obtained for all other uses, in any current or future media, including reprinting/republishing this material for advertising or promotional purposes, creating new collective works, for resale or redistribution to servers or lists, or reuse of any copyrighted component of this work in other works. DOI: 10.1109/ACSSC.2012.6488983

zero subcarriers at the band edges and at DC. As a consequence of this setup, both systems showed almost the same bandwidth efficiency, however, they differed in terms of the theoretical achievable data rate. Nevertheless, considering that bandwidth is an expensive resource when talking about real-world communication systems, this seems to be a reasonable and fair comparison. In this paper we compare from a different point of view and investigate UW-OFDM and CP-OFDM configurations that show the same theoretical data rate. As a consequence, the two systems differ in subcarrier spacing, DFT size and DFT period. Moreover, in this work we also highlight the similarities between non-systematic coded UW-OFDM and unique word based single carrier/frequency domain equalization (UW-SC/FDE) systems.

*Notation:* Lower-case bold face variables ( $\mathbf{a}, \mathbf{b}, \dots$ ) indicate vectors, and upper-case bold face variables ( $\mathbf{A}, \mathbf{B}, \dots$ ) indicate matrices. To distinguish between time and frequency domain variables, we use a tilde to express frequency domain vectors and matrices ( $\tilde{\mathbf{a}}, \tilde{\mathbf{A}}, \dots$ ), respectively. We further use  $\mathbb{R}$  to denote the set of real numbers,  $\mathbb{C}$  to denote the set of complex numbers,  $\mathbf{I}$  to denote the identity matrix,  $(\cdot)^T$  to denote transposition,  $(\cdot)^H$  to denote conjugate transposition,  $E[\cdot]$  to denote expectation, and  $\text{tr}\{\cdot\}$  to denote the trace operator. For all signals and systems the usual equivalent complex baseband representation is applied.

## II. REVIEW OF NON-SYSTEMATIC CODED UW-OFDM

We briefly review our approach of introducing unique words in OFDM time domain symbols, for further details see [6]. Let  $\mathbf{x}_u \in \mathbb{C}^{N_u \times 1}$  be a predefined sequence which we call unique word. This unique word shall form the tail of each OFDM time domain symbol vector. Hence, an OFDM time domain symbol vector, as the result of a length- $N$ -IDFT (inverse DFT), consists of two parts and is of the form  $[\mathbf{x}_d^T \ \mathbf{x}_u^T]^T \in \mathbb{C}^{N \times 1}$ , whereat only  $\mathbf{x}_d \in \mathbb{C}^{(N-N_u) \times 1}$  is random and affected by the data. Following [3], we generate an OFDM symbol  $\mathbf{x} = [\mathbf{x}_d^T \ \mathbf{0}^T]^T$  with a zero UW in a first step, and we determine the final transmit symbol  $\mathbf{x}' = \mathbf{x} + [\mathbf{0}^T \ \mathbf{x}_u^T]^T$  by adding the desired UW in time domain in a second step. As in conventional OFDM, the QAM data symbols (denoted by the vector  $\tilde{\mathbf{d}} \in \mathbb{C}^{N_d \times 1}$ ) and the zero subcarriers (at the band edges and at DC) are specified in frequency domain as part of the vector  $\tilde{\mathbf{x}}$ , but here in addition the zero-word is specified in time domain as part of the vector  $\mathbf{x} = \mathbf{F}_N^{-1} \tilde{\mathbf{x}}$ . Here,  $\mathbf{F}_N$  denotes the length- $N$ -DFT matrix with elements  $[\mathbf{F}_N]_{kl} = e^{-j\frac{2\pi}{N}kl}$  for  $k, l = 0, 1, \dots, N-1$ . The system of equations  $\mathbf{x} = \mathbf{F}_N^{-1} \tilde{\mathbf{x}}$  with the introduced features can be fulfilled by defining a code word  $\tilde{\mathbf{c}} \in \mathbb{C}^{(N_d+N_r) \times 1}$  with  $N_r = N_u$ , and an appropriate generator matrix  $\mathbf{G}$  such that  $\tilde{\mathbf{c}} = \mathbf{G} \tilde{\mathbf{d}}$  with  $\mathbf{G} \in \mathbb{C}^{(N_d+N_r) \times 1}$  fulfilling

$$\mathbf{F}_N^{-1} \mathbf{B} \mathbf{G} \tilde{\mathbf{d}} = \begin{bmatrix} \mathbf{x}_d \\ \mathbf{0} \end{bmatrix} \quad (1)$$

for every possible data vector  $\tilde{\mathbf{d}}$ , or equivalently

$$\mathbf{F}_N^{-1} \mathbf{B} \mathbf{G} = \begin{bmatrix} * \\ \mathbf{0} \end{bmatrix}. \quad (2)$$

Here,  $\mathbf{B} \in \mathbb{C}^{N \times (N_d+N_r)}$  models the insertion of zero subcarriers and becomes identity in case no zero subcarriers are introduced.

In our original UW-OFDM concept presented in [1], [2], [3], we chose  $\mathbf{G}$  such that  $\mathbf{G} = \mathbf{P} [\mathbf{I} \ \mathbf{T}^T]$ , leading to dedicated data and dedicated redundant subcarriers, the latter responsible for creating the desired zero UW in the time domain. Here,  $\mathbf{P} \in \mathbb{C}^{(N_d+N_r) \times (N_d+N_r)}$  denotes a permutation matrix and  $\mathbf{T} = -\mathbf{M}_{22}^{-1} \mathbf{M}_{21} \in \mathbb{C}^{N_r \times N_d}$  creates the redundancy, whereas  $\mathbf{M}_{ij}$  are appropriately sized sub-matrices originating from  $\mathbf{M} = \mathbf{F}_N^{-1} \mathbf{B} \mathbf{P} = \begin{bmatrix} \mathbf{M}_{11} & \mathbf{M}_{12} \\ \mathbf{M}_{21} & \mathbf{M}_{22} \end{bmatrix}$ . Since data and redundancy symbols are clearly distinguishable, we refer to this approach as systematic coded UW-OFDM.

Recently, we introduced in [6] the so-called *non-systematic* coded UW-OFDM concept, where we now propose a code generator matrix  $\check{\mathbf{G}}$  that distributes the redundancy and data symbols over several subcarriers. For that we model the code generator matrix as

$$\check{\mathbf{G}} = \mathbf{A} \mathbf{P} \begin{bmatrix} \mathbf{I} \\ \check{\mathbf{T}} \end{bmatrix}, \quad (3)$$

with a non-singular real matrix  $\mathbf{A} \in \mathbb{R}^{(N_d+N_r) \times (N_d+N_r)}$  and a fixed permutation matrix, e.g. obtained from the systematic coded UW-OFDM approach. The constraint in (2) can thus be re-written as

$$\mathbf{F}_N^{-1} \mathbf{B} \mathbf{A} \mathbf{P} \begin{bmatrix} \mathbf{I} \\ \check{\mathbf{T}} \end{bmatrix} = \begin{bmatrix} * \\ \mathbf{0} \end{bmatrix}. \quad (4)$$

With the introduction of

$$\check{\mathbf{M}} = \mathbf{F}_N^{-1} \mathbf{B} \mathbf{A} \mathbf{P} = \begin{bmatrix} \check{\mathbf{M}}_{11} & \check{\mathbf{M}}_{12} \\ \check{\mathbf{M}}_{21} & \check{\mathbf{M}}_{22} \end{bmatrix}, \quad (5)$$

the constraint in (4) is simply and automatically fulfilled by choosing  $\check{\mathbf{T}}$  as

$$\check{\mathbf{T}} = -(\check{\mathbf{M}}_{22})^{-1} \check{\mathbf{M}}_{21}. \quad (6)$$

In [6] we aimed at finding a generator matrix  $\check{\mathbf{G}}$  that minimizes the sum of the error variances on the subcarriers after a linear minimum mean square error (LMMSE) data estimator [7]. We model the receive symbol  $\tilde{\mathbf{y}} \in \mathbb{C}^{(N_d+N_r) \times 1}$  (after subtraction of the UW related portion  $\tilde{\mathbf{H}} \mathbf{B}^T \mathbf{F}_N [\mathbf{0}^T \ \mathbf{x}_u^T]^T$ ) as

$$\tilde{\mathbf{y}} = \tilde{\mathbf{H}} \check{\mathbf{G}} \tilde{\mathbf{d}} + \tilde{\mathbf{v}}, \quad (7)$$

whereas the diagonal matrix  $\tilde{\mathbf{H}} \in \mathbb{C}^{(N_d+N_r) \times (N_d+N_r)}$  contains the sampled channel frequency response on its main diagonal,  $\tilde{\mathbf{v}} = \mathbf{B}^T \mathbf{F}_N \mathbf{n}$  with  $\mathbf{n} \in \mathbb{C}^{N \times 1}$  represents a zero-mean Gaussian (time domain) noise vector with the covariance matrix  $\sigma_n^2 \mathbf{I}$ , and  $\tilde{\mathbf{d}} \in \mathbb{C}^{N_d \times 1}$  denotes a QAM data symbol vector with the covariance matrix  $\sigma_d^2 \mathbf{I}$ . It can easily be shown (for more details we refer again to [6]) that the cost function to be minimized follows to

$$J_{\text{LMMSE}} = \frac{\sigma_d^2}{cN_d} \text{tr}\{\check{\mathbf{G}}^H \check{\mathbf{G}}\} \text{tr} \left\{ \left( \check{\mathbf{G}}^H \check{\mathbf{G}} + \frac{\text{tr}\{\check{\mathbf{G}}^H \check{\mathbf{G}}\}}{cN_d} \mathbf{I} \right)^{-1} \right\}. \quad (8)$$

Here, we assumed AWGN conditions by choosing  $\tilde{\mathbf{H}} = \mathbf{I}$  in order to avoid the dependence of the optimum generator matrix on the specific channel instance, and additionally fixed

the ratio  $c = E_s/\sigma_n^2$  whereas the mean QAM data symbol energy  $E_s$  follows to  $E_s = \frac{\sigma_n^2}{N} \text{tr}\{\check{\mathbf{G}}^H \check{\mathbf{G}}\}/N_d$ .

We use the steepest descent algorithm to numerically solve the optimization problem. For that the gradient of the cost function  $J_{\text{LMMSE}}$  with respect to the real matrix  $\mathbf{A}$  is required. We approximate the partial derivation  $\partial J_{\text{LMMSE}}/\partial[A]_{ij}$  by

$$\frac{\partial J_{\text{LMMSE}}}{\partial[A]_{ij}} = \frac{J_{\text{LMMSE}}([A]_{ij} + \epsilon) - J_{\text{LMMSE}}([A]_{ij} - \epsilon)}{2\epsilon} \quad (9)$$

with a very small  $\epsilon$ . We apply two different approaches for the initialization of the steepest descent algorithm:

In our first approach we choose the initialization  $\mathbf{A}^{(0)} = \mathbf{I}$  which implies  $\mathbf{T}^{(0)} = \mathbf{T}$  and

$$\check{\mathbf{G}}^{(0)} = \mathbf{P} [\mathbf{I} \quad \mathbf{T}^T]^T = \mathbf{G}. \quad (10)$$

The iterative optimization process consequently starts with the code generator matrix  $\mathbf{G}$  of our original systematic coded UW-OFDM concept, which can definitely be assumed to be a good initial guess. We denote the resulting optimum code generator matrix (found after convergence of the algorithm) with  $\check{\mathbf{G}}'$ .

In the second approach we choose each element of  $\mathbf{A}^{(0)}$  as a realization of a Gaussian random variable with mean zero and variance one such that  $[A^{(0)}]_{ij} \sim \mathcal{N}(0, 1)$ . We denote the resulting code generator matrix with  $\check{\mathbf{G}}''$ . Due to the random initialization, the resulting code generator matrix generally varies from trial to trial. For our simulations, we will use for each of the investigated parameter setups (see Table I) one particular realization of  $\check{\mathbf{G}}''$ .

It turns out that the initialization of  $\mathbf{A}$  in the optimization algorithm highly influences the structure of the resulting code generator matrix and thus also the resulting performance. We will detail this in the next section.

### III. SIMULATIONS

We have already shown the advantageous properties of the proposed UW-OFDM concept over a conventional CP-OFDM system in former papers, cf. [2], [6]. However, when evaluating two different concepts against each other, there are always several ways of how to compare both systems. Up till now, we have focused on practical scenarios and chose the IEEE 802.11a WLAN standard as a classical CP-OFDM reference system. As such, we used the same configuration as in [8] whenever possible, the most important parameters are summarized in Table I and referred to as *CP-OFDM I* and *UW-OFDM I*. Keeping the DFT size and the sampling frequency of  $f_s = 20$  MHz constant, it turns out that the UW-OFDM system differs from the IEEE 802.11a system in the OFDM symbol duration and the number of data subcarriers per OFDM symbol. The latter is due to the fact that additional subcarriers are required to introduce the redundancy needed for creating the desired UW in the time domain. Because of that the CP-OFDM system provides a 6.67% higher theoretical data rate (additional overhead like e.g. a preamble for estimation and synchronization tasks are not considered here) than the UW-OFDM system. Although UW-OFDM achieves a lower data rate on one hand, it requires less bandwidth on the other hand, thus both systems show almost the same bandwidth efficiency.

Hence, this seems to be a reasonable and fair comparison considering that bandwidth is an expensive resource, especially w.r.t. real-world communication scenarios.

In this paper we again compare our UW-OFDM concept with conventional CP-OFDM, however, now we design the systems such that both offer the same theoretical data rate, cf. the columns *CP-OFDM II* and *UW-OFDM II* in Table I. Moreover, in this work we focus on the principle capabilities of both concepts and thus neglect typical features of a practical OFDM system like e.g. zero subcarriers. As we furthermore omit pilot subcarriers for the CP-OFDM system, we also choose the zero word as UW in case of the UW-OFDM system. For a DFT size of 64, the CP-OFDM allows to transmit 64 data symbols within an OFDM symbol duration of  $4\mu\text{s}$ . In order to achieve the same data rate for the UW-OFDM concept, we enlarge the DFT size to 80 and the DFT period (and thus also the OFDM symbol duration) to  $4\mu\text{s}$ . Hence, both systems provide the same theoretical data rate, but now differ in the DFT size, DFT period and consequently also in subcarrier spacing. We note that an enlarged DFT size has basically no impact on the resulting complexity, as in UW-OFDM the complexity at the transmitter and the receiver side are dominated by other operations, cf. [1].

We use the same simulation chain as described in [6]. Hence, the transmitter processing starts with (outer) channel coding, interleaving and QPSK mapping. We utilize the same outer convolutional encoder as defined in [8], and show results for (outer) coding rates  $r = 1/2$  and  $r = 3/4$ , respectively. Next, we generate the OFDM symbol by applying  $\check{\mathbf{G}}'$  or  $\check{\mathbf{G}}''$ , respectively, and perform the IFFT. At the receiver side, we start with an FFT and then apply an LMMSE data estimation. Finally, demapping, deinterleaving and decoding is performed. For the soft decision Viterbi decoder the main diagonal of the LMMSE error covariance matrix is used to specify the varying noise variances along the subcarriers after data estimation. Perfect channel knowledge is assumed at the receiver.

The following BER results have been obtained by averaging over  $10^4$  channel realizations whereas each channel impulse response has been normalized such that the receive power is independent of the actual channel. The channel impulse responses have been modelled as tapped delay lines, each tap with uniformly distributed phase and Rayleigh distributed magnitude, and with power decaying exponentially, cf. [9].

Fig. 2 shows the BER behavior of the CP-OFDM and the UW-OFDM system when transmitting over channels featuring a channel delay spread of 100 ns. We notice that for both (outer) coding rates, the two UW-OFDM approaches always outperform the CP-OFDM system (measured at a BER of  $10^{-6}$ ). Whereas the UW-OFDM system utilizing  $\check{\mathbf{G}}''$  as code generator matrix achieves only a marginal gain of 0.1dB in case of  $r = 1/2$ , this gain increases to 1.1dB when  $\check{\mathbf{G}}'$  is applied. For an (outer) coding rate of  $r = 3/4$ , both systems outperform the conventional CP-OFDM concept remarkably, namely by 3dB and 2dB at a BER of  $10^{-6}$ , respectively.

Fig. 3 compares the UW-OFDM concept with the CP-OFDM system when transmitting over multipath channels featuring a channel delay spread of 200 ns. We again observe

TABLE I  
MAIN PHY PARAMETERS OF THE INVESTIGATED SYSTEMS.

	CP-OFDM I	UW-OFDM I	CP-OFDM II	UW-OFDM II	UW-OFDM III
DFT size	64	64	64	80	64
Occupied subcarriers	52	52	64	80	64
Data symbols	48	36	64	64	48
Additional symbols	4 (pilot)	16 (redundant)	0	16 (redundant)	16 (redundant)
DFT period	3.2 $\mu$ s	3.2 $\mu$ s	3.2 $\mu$ s	4 $\mu$ s	3.2 $\mu$ s
Guard duration	800 ns (CP)	800 ns (UW)	800 ns (CP)	800 ns (UW)	800 ns (UW)
Total OFDM symbol duration	4 $\mu$ s	3.2 $\mu$ s	4 $\mu$ s	4 $\mu$ s	3.2 $\mu$ s
Subcarrier spacing	312.5 kHz	312.5 kHz	312.5 kHz	250 kHz	312.5 kHz

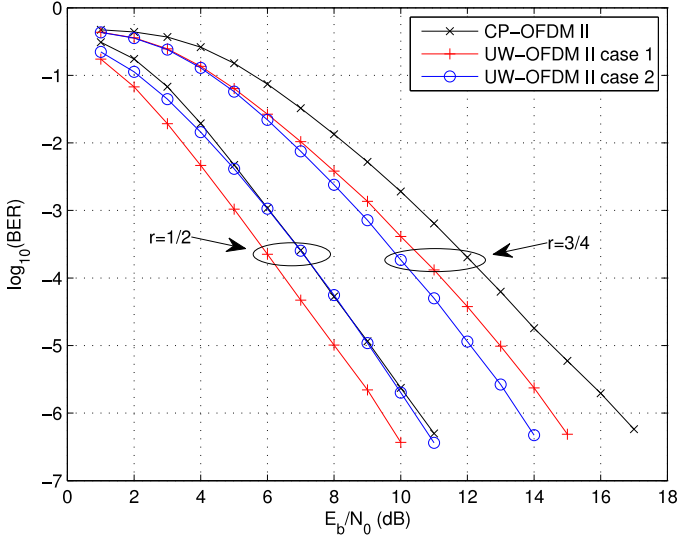


Fig. 2. BER results for UW-OFDM ( $\check{G}'$  and  $\check{G}''$ ) and CP-OFDM for multipath channels with a delay spread of 100 ns.

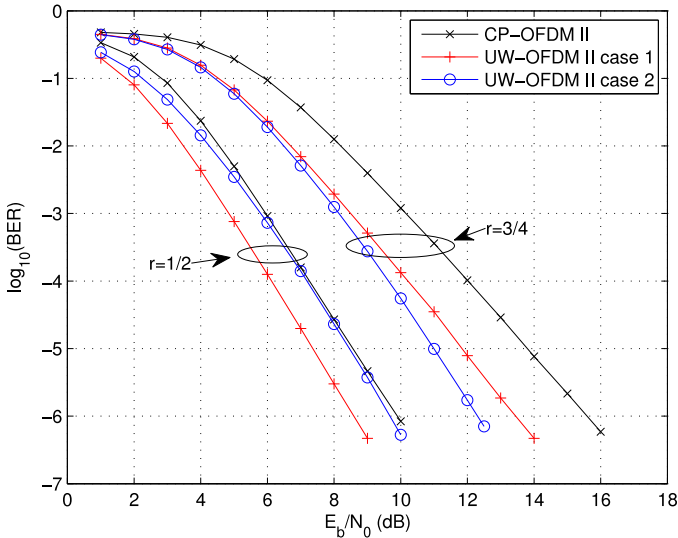


Fig. 3. BER results for UW-OFDM ( $\check{G}'$  and  $\check{G}''$ ) and CP-OFDM for multipath channels with a delay spread of 200 ns.

the same tendencies. The UW-OFDM approaches outperform the CP-OFDM system by 0.2 and 1.3dB in case of  $r = 1/2$  and by 3.3dB and 2.1dB in case of  $r = 3/4$ , respectively.

We note that in general UW-OFDM concepts with a code generator matrix  $\check{G}'$  always outperform UW-OFDM systems

applying  $\check{G}''$  in case of low (outer) coding rates, and the situation is contrary in case of high (outer) coding rates. This is due to the fact that  $\check{G}'$  only spreads a data symbol over a few local subcarriers and thus works similar to a conventional OFDM system, while  $\check{G}''$  spreads a data symbol over many (or even all) subcarriers and thus acts like a classical single carrier system. Keeping in mind that a single carrier based system outperforms an OFDM based system for high outer coding rates, whereas it is vice versa in case of low (outer) coding rates, these effects become reasonable. In [6] we have already noted that UW-SC/FDE can be seen as a special case of non-systematic coded UW-OFDM with a generator matrix

$$\check{G}_{SC} = \mathbf{F}_N \begin{bmatrix} \mathbf{I} \\ \mathbf{0} \end{bmatrix}. \quad (11)$$

Fig. 4 compares the BER behavior of UW-OFDM using our particular chosen  $\check{G}''$  and  $\check{G}_{SC}$  for the setup *UW-OFDM III* in Table I. We immediately notice that both concepts in fact achieve the same BER performance.

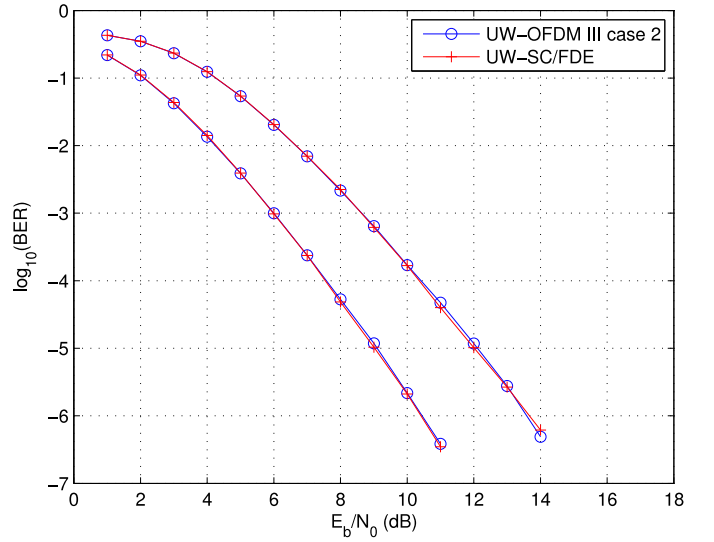


Fig. 4. BER results for UW-OFDM ( $\check{G}'$ ) and UW-SC/FDE ( $\check{G}_{SC}$ ) for multipath channels with a delay spread of 100 ns.

#### IV. CONCLUSION

In this paper we compared the BER behavior of the non-systematic coded UW-OFDM concept against conventional CP-OFDM. In contrast to previous papers, we have now designed the UW-OFDM and CP-OFDM system such that they

achieve the same theoretical data rate. We have demonstrated that again the UW-OFDM approach remarkably outperforms CP-OFDM. Furthermore, it turns out that an UW-OFDM system performs like an UW-SC/FDE system when choosing an appropriate code generator matrix.

#### REFERENCES

- [1] M. Huemer, A. Onic, C. Hofbauer, "Classical and Bayesian Linear Data Estimators for Unique Word OFDM," in the *IEEE Transactions on Signal Processing*, vol. 59, no. 12, pp. 6073-6085, Dec. 2011.
- [2] M. Huemer, C. Hofbauer, J.B. Huber, "The Potential of Unique Words in OFDM," in the *Proceedings of the 15th International OFDM-Workshop*, Hamburg, Germany, pp. 140-144, September 2010.
- [3] A. Onic, M. Huemer, "Direct versus Two-Step Approach for Unique Word Generation in UW-OFDM," in the *Proceedings of the 15th International OFDM-Workshop*, Hamburg, Germany, pp.145-149, September 2010.
- [4] R. van Nee, R. Prasad, *OFDM for Wireless Multimedia Communications*, Artech House Publishers, Boston, 2000.
- [5] S. Tang, F. Yang, K. Peng, C. Pan, K. Gong, Z. Yang, "Iterative channel estimation for block transmission with known symbol padding - a new look at TDS-OFDM," in the *Proceedings of the IEEE Global Telecommunications Conference (GLOBECOM 2007)*, pp. 4269-4273, Nov. 2007.
- [6] M. Huemer, C. Hofbauer, J. B. Huber, "Non-Systematic Complex Number RS Coded OFDM by Unique Word Prefix," in the *IEEE Transactions on Signal Processing*, vol. 60, no. 1, pp. 285-299, Jan 2012.
- [7] S. Kay, *Fundamentals of Statistical Signal Processing: Estimation Theory*, Prentice Hall, Rhode Island 1993.
- [8] IEEE Std 802.11a-1999, Part 11: Wireless LAN Medium Access Control (MAC) and Physical Layer (PHY) specifications: High-Speed Physical Layer in the 5 GHz Band, 1999.
- [9] J. Fakatselis, Criteria for 2.4 GHz PHY Comparison of Modulation Methods. Document IEEE 1997; P802.11-97/157r1.